Electron energy loss spectroscopy of the $L_{2,3}$ edge of phosphorus skutterudites and electronic structure calculations

Ragnhild Sæterli,[1] Espen Flage-Larsen,[2] Øystein Prytz,[2] Johan Taftø,[2] Knut Marthinsen,[3] and Randi Holmestad[1,*]
[1]*Department of Physics, Norwegian University of Science and Technology (NTNU), 7491 Trondheim, Norway*
[2]*Department of Physics, University of Oslo, P.O. Box 1048, NO-0316 Oslo, Norway*
[3]*Department of Materials Science and Engineering, Norwegian University of Science and Technology (NTNU), 7491 Trondheim, Norway*
(Received 24 April 2009; revised manuscript received 2 July 2009; published 11 August 2009)

In this study we report the results of experiments and theoretical calculations on the phosphorus $L_{2,3}$ edges of the skutterudites CoP_3, $LaFe_4P_{12}$, NiP_3, RhP_3, and IrP_3. Phosphorus *s* and *d* density of states above the Fermi level was studied by transmission electron energy loss spectroscopy while theoretical calculations were performed using both a real-space multiple-scattering procedure and density-functional theory. Generally, there are good agreements between both types of calculations and the experimental results. The near-edge structure of all the examined compounds shows the same overall features, including the metallic NiP_3 and the metallic filled skutterudite $LaFeP_{12}$, and is well explained by comparison to phosphorus density of states. We also discuss the similarities to previously reported results on Si $L_{2,3}$ edges and interpret the differences of the various skutterudites in terms of the electronegativities of the involved atom species.

DOI: 10.1103/PhysRevB.80.075109 PACS number(s): 71.20.Nr, 71.15.Mb, 79.20.Uv, 72.20.Pa

I. INTRODUCTION

The binary skutterudites MX_3 (M=Co, Rh, Ir, and Ni; X=P, As, and Sb) have received particular attention as promising candidates for good thermoelectric performance. Their crystal structure is the same as that of the mineral $CoAs_3$ from which the skutterudite name has been adopted and consists of corner-sharing X octahedra centered on an M atom. These octahedra are tilted to form nearly square X_4 rings and large voids that can be filled by rare-earth atoms, obtaining the ternary or filled skutterudites. As is depicted in Fig. 1, the X atoms are tetrahedrally or semi-tetrahedrally coordinated with two nearest X atoms and two M atoms. The filler atoms significantly increase the phonon scattering due to the supposedly uncorrelated motion of the filler atoms. However, recent studies[1,2] suggest a more correlated motion and that the main reason for the reduction in thermal conductivity is due to phonon band flattening. The lowering of thermal conductivity is vital to a good thermoelectric performance and thus a variety of filling atoms and degrees of fillings have been tested for thermoelectric properties.[3–6] Substitution both on metal and pnictide sites[7,8] has revealed that an additional reduction in thermal conductivity can be achieved and even small amounts of impurity atoms are found to affect the electronic properties and band structure of $CoSb_3$.[9]

So far, most investigations of the electronic structure of skutterudites have been theoretical calculations. One of the first skutterudite band-structure calculations was done by Jung *et al.*[10] By the use of tight-binding calculations they examined the metallic $LaFe_4P_{12}$ and concluded that the highest occupied energy band is dominated by phosphorus 3*s* and 3*p* states. In light of this they proposed that electronic and magnetic properties are mainly determined by the behavior of the phosphorus rings. Llunell *et al.*[11] showed through the use of scalar-relativistic linear muffin-tin orbital calculations that the same behavior is present for CoP_3 and NiP_3. They also predicted CoP_3 to be a narrow band-gap semiconductor. Later, Fornari and Singh[12] reported semi-metallic CoP_3 through the use of density-functional theory calculations. Lefebvre-Devos *et al.*[13] showed in a combined density of state and charge-density study that the tilted corner-connected MX_6 octahedra gave the main features of the highest valence band. Two different density-functional theory approaches were applied by Løvvik and Prytz,[14] both supporting a more metallic conduction in CoP_3. Semimetallic behavior of CoP_3 was also shown by Takegahara *et al.*,[15] again by the use of density-functional theory. In the same work they investigated IrP_3 and RhP_3 and found that IrP_3 was a semiconductor while RhP_3 was a semi-metal. Beyond what has been suggested by Uher *et al.*[16] and Nolas *et al.*,[3] there have been few studies addressing the charge distribution in skutterudite compounds.

Of the few experimental investigations on electronic structure of skutterudites is the work of Grosvenor *et al.*[17,18] and Diplas *et al.*[19] performing x-ray photoemission spectra

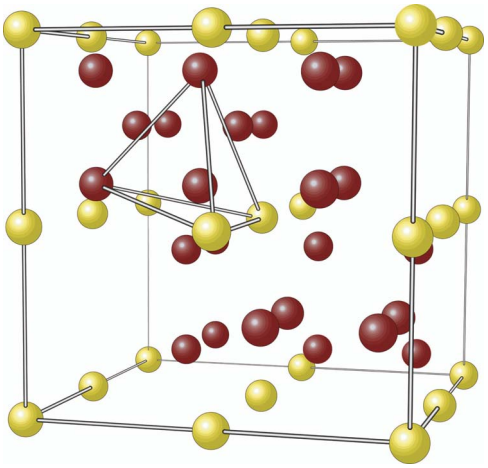

FIG. 1. (Color online) The unfilled skutterudite structure. Phosphorus and transition metals are depicted as dark (red) and bright (yellow), respectively. The semi-tetrahedral arrangement of a phosphorus atom is shown with lines.

(XPS) on various skutterudites including CoP_3 and $LaFe_4P_{12}$. Prytz *et al.*[20] studied the transition-metal L edges by electron energy loss spectroscopy (EELS) in a series of skutterudites including CoP_3, NiP_3, and $LaFe_4P_{12}$, concluding that there was a significant depletion of $3d$ M electrons in the binary phosphorus skutterudites. They suggested that the reason was hybridization of valence states, rather than charge transfer. In $LaFe_4P_{12}$, they proposed that the electrons donated by La^{3+} was solely taken up by Fe.

The phosphorus skutterudites are not as extensively studied as their Sb counterparts, due to their poorer thermoelectric performance. However, the electronegativity differences are larger in the P compounds, making any charge transfer easier to identify and thereby simplifying the task of investigating their electronic structure before proceeding to Sb skutterudites. In addition, the ambiguities and unresolved questions arising both from theoretical and experimental investigations need to be further investigated.

Though not much used on skutterudites, EELS and, in particular, energy loss near-edge spectroscopy (ELNES) are well-established techniques for examining the electronic structure in materials.[21] Well-known examples include examination of valence state[22] and determination of local environment of the studied atom site.[23] The latter is usually obtained through a "fingerprint"[24] recognition of the specific phases involved since a quantitative analysis of the near-edge structure is not straightforward.

Few EELS investigations of P in crystalline materials have been published. Some works have been reported on P in biological specimens,[25,26] however these papers mainly involve detection limits and quantization of minute amounts of the element. Garvie and Buseck[27] and Miao *et al.*[28] used the P $L_{2,3}$ ELNES spectrum from apatite and triphylite, respectively, both containing PO_4 tetrahedra. Here, we report the results of an ELNES investigation of several phosphorus skutterudites with P also in tetrahedral environments, but with other ligands, and show that these give a fine structure very different from that of PO_4-containing crystals. We also compare the experimental spectra to spectra modeled using a real-space multiple-scattering (RSMS) approach and density-of-states (DOS) calculations performed using density-functional theory (DFT) in order to interpret the features and draw conclusions on the electronic structure of these skutterudites.

II. EXPERIMENTAL PROCEDURES AND CALCULATIONS

A. Materials

Samples of CoP_3, $LaFe_4P_{12}$, and NiP_3 were synthesized using the tin-flux technique described by Jeitschko[29] and Watcharapasorn.[30] The tin flux was dissolved in dilute hydrochloric acid, leaving single crystals which were analyzed by x-ray diffraction (XRD). For CoP_3 and NiP_3, no sign of other phases were detected. However, secondary phases were detected for the nominal $LaFe_4P_{12}$ samples. The RhP_3 and IrP_3 compounds were synthesized by direct reaction of stoichiometric amounts of the constituent elements in sealed and evacuated silica ampoules.

Transmission electron microscopy (TEM) specimens were prepared by crushing particles in ethanol which were left to dry on a TEM copper grid with amorphous holey carbon film. XRD as well as electron-diffraction and energy-dispersive x-ray spectroscopy were used to check structure and composition of the produced batch and individual particles used for EELS analysis.

B. ELNES

EELS and ELNES are powerful techniques that are able to give important insight into the electronic structure of materials. The basic principle is that as electrons are transmitted through the sample, some of them loose energy by inelastic collisions on their way. The energy of the transmitted electrons is then measured and an energy spectrum is formed. One of the inelastic processes is core losses, in which an electron in an atomic core level is excited to an empty state above the Fermi energy. As the core states are localized in energy, the energy spread above such a core-loss edge is directly dependent on the number of available final states, making bonding effects visible. The observed intensity is dependent on the DOS and a matrix element dictating that usually only excitations with a change in angular momentum Δl of ± 1 is allowed. Furthermore, excitations are spatially limited so that initial and final states are localized on the same atom. Hence, ELNES is said to measure a site- and symmetry-projected DOS.[21]

Control of the experimental parameters is vital to any quantitative or qualitative EELS work. The ELNES spectra in this study were all taken at a JEOL 2010F with a Gatan-Imaging Filter attached, operated at 200 kV in convergent-beam diffraction mode with a beam convergence of about 5 mrad and a collection angle of about 9 mrad. Convergent-beam mode was chosen to ensure consistency in the results, as a parallel beam was found to give too much variation between the acquired spectra and thus inconsistent results, probably due to sample thickness changes within the examined sample area. For the same reason diffraction mode (image coupling) was used, as it is well known that imaging mode is more prone to erroneous interpretation.[21] The energy resolution of all spectra is comparable and about 1 eV, measured as the full width at half maximum of the zero-loss peak. All spectra were recorded on a dark current subtracted and gain-corrected charge-coupled device with an energy dispersion of 0.1 eV/channel. The background in all spectra has been subtracted by fitting an exponentially decaying function to an energy window of 10 eV just before the edge onset. Spectra were acquired from areas of a thickness of 0.2–0.5 mean-free paths and were deconvoluted using the Fourier-ratio method in DIGITALMICROGRAPH and a low-loss spectrum from the same area of the specimen, taken shortly before or after the core-loss spectrum. A sum of several spectra from each material was used for better counting statistics and care was taken to avoid strong channelling conditions. No attempts were made to measure the absolute edge onset of the materials, thus the onsets have been shifted to match those of the calculated spectra.

For $LaFe_4P_{12}$, the La $N_{4,5}$ edge at approximately 100 eV was subtracted using a perovskite $LaCoO_3$ specimen to

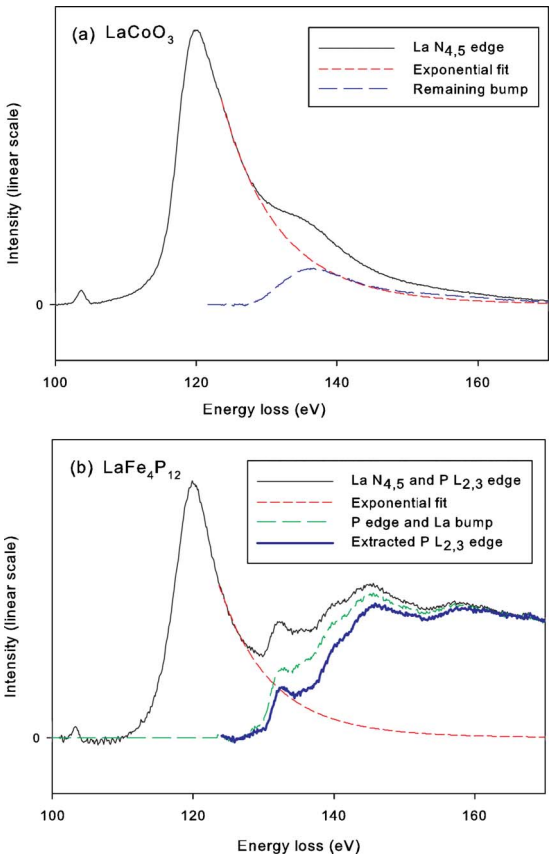

FIG. 2. (Color online) (a) Experimental $LaCoO_3$ La $N_{4,5}$ edge (thin solid/black line) used for subtracting the La edge from $LaFe_4P_{12}$ and (b) $LaFe_4P_{12}$ P $L_{2,3}$ edge before (thin solid/black line) and after (thick solid/blue line) subtracting the La $N_{4,5}$ edge. The edge was extracted by fitting an exponential (short-dashed/red line) to the right-hand side of the La peak in both spectra and then normalizing and subtracting the rest from the $LaCoO_3$ spectrum (long-dashed/blue line) from the $LaFe_4P_{12}$ spectrum.

record the pure La edge as illustrated in Fig. 2. Both the perovskite and the skutterudite structure have tilted O/P octahedra and the La atoms are enclosed in an irregular dodecahedron of O/P atoms.[31] The main La edge of $LaCoO_3$ is broader than in $LaFe_4P_{12}$, probably due to more tightly bound La atoms in the perovskite as compared to the skutterudite, where the La atoms are more weakly bound "rattlers." Thus, the La edge was subtracted by fitting an exponential function to the high-energy side of the La peak in both the perovskite and the skutterudite spectrum, leaving a residual intensity at approximately 135 eV in the perovskite spectrum. This intensity was then normalized and subtracted from the $LaFe_4P_{12}$ spectrum as depicted in Fig. 2.

C. Real-space multiple-scattering calculations

The experimental L edges were compared to spectra modeled using the RSMS code Feff8.[32] In these calculations, self-consistent muffin-tin potentials were obtained using Hedin-Lundqvist local-density approximation self-energies.[33] Potentials were calculated with and without a core hole in the $2p$ shell of the central atom. Spectra modeled in the presence of a core hole gave better correspondence with the experiments and all spectra presented here were calculated with a core hole. An angular-momentum basis with $l=3$ (f electrons) was used in the calculations for the La-, Rh-, and Ir-containing compounds. Calculations with angular momenta up to $l=4$ were also tested, with only minor changes in the resulting spectra. The convergence of the calculated spectra with respect to cluster size were tested for clusters up to 700 atoms in CoP_3 but all the main spectral features were reproduced for clusters as small as 150 atoms. Similar results were obtained for the other compounds. The spectra presented here are calculated for clusters of about 180 atoms. Although the Fermi level and final-state energies are found in the self-consistent-field calculations, Feff8 has no means of determining the initial-state binding energies, apart from assuming that they are equal to those of the free-atom values, which are the values used in the presented spectra.

D. Density-functional calculations

To go beyond the approximation made in the RSMS approach, DFT calculations in the generalized-gradient approximation[34–37] were performed. The highly efficient projector-augmented wave[38,39] method was used along with Perdew-Burke-Ernzerhof[40] exchange-correlation functionals. All calculations were done using the Vienna *ab initio* simulation package (VASP).[39,41–45] Structures were relaxed both in cell size, shape, and atomic positions, using the residual minimization scheme, direct inversion in the iterative subspace (RMM-DIIS) (Ref. 46) algorithm. During the relaxation a Gaussian smearing[47] of 0.05 eV was used for all structures. After the relaxation another self-consistent calculation was done to ensure correct representation of the system. An energy cutoff of 800 eV for $LaFe_4P_{12}$ and 550 eV for all other structures, was necessary to obtain proper convergence of the total energy to within 2 meV. A k-point grid of $8\times8\times8$ was sufficient to achieve similar convergence. To obtain accurate DOS the tetrahedron method with Blöchl corrections[48] was used. Literature values[49] for the covalent radii were used to generate the partial DOS.

III. RESULTS AND DISCUSSION

Figure 3 shows the experimental P $L_{2,3}$ edges of CoP_3, $LaFe_4P_{12}$, NiP_3, IrP_3, and RhP_3, respectively, (solid lines), with the edge onsets shifted and experimental intensities scaled to match the RSMS calculations (dashed lines). The edges of the binary skutterudites are very similar, consisting of an initial peak (denoted A in Fig. 3) indicating the edge onset at about 125 eV, and additional peaks (B and C) extending up to above 140 eV.

As is easily observed, the RSMS simulations are able to reproduce the overall shape of the experimental P $L_{2,3}$ edges as well as the position of the peaks for all of the studied compounds. Moreover, the fit is clearly better for the lighter element binary skutterudites than their Ir and Rh counterparts. The overall fit suggests that the bonding in skutterudite compounds is accurately described in the RSMS calcula-

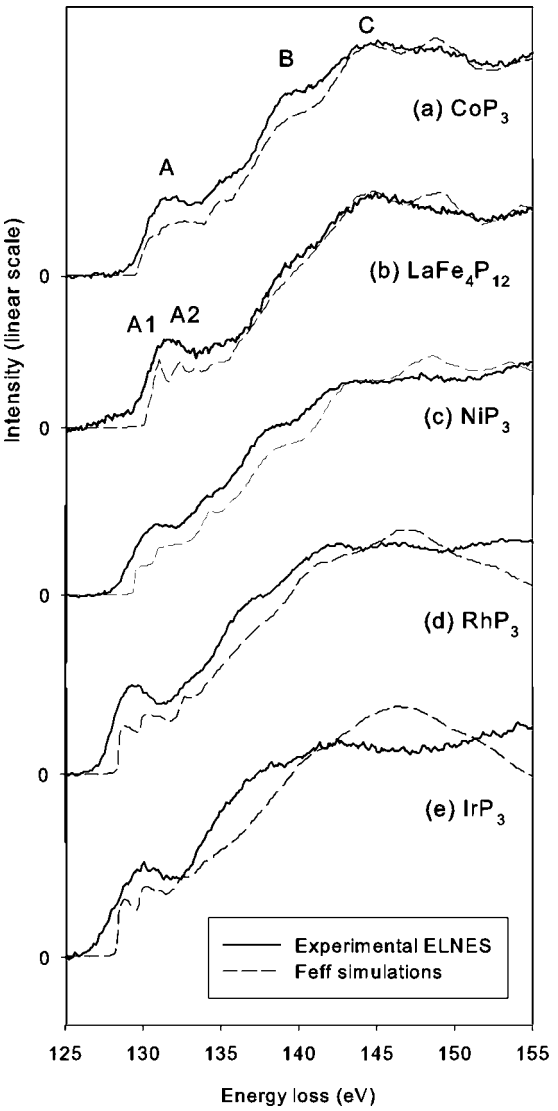

FIG. 3. Experimental P edges (solid lines) compared to edges simulated by Feff8 (dashed lines) with core hole for (a) CoP_3, (b) $LaFe_4P_{12}$, (c) NiP_3, (d) RhP_3, and (e) IrP_3.

tions, in contrast to previously reported results on the pure phosphorus compound.[50]

Comparing with EELS spectra recorded from pure Si (see, e.g., Ref. 51), the same overall edge shape is found. This fact reflects the similar bonding arrangement of elemental Si compared to P in skutterudites: In a binary skutterudite MP_3, each P atom bonds to two other P atoms and two *M* atoms. The two *X*-*X* bonds in skutterudites are of different length (2.24 and 2.34 Å in CoP_3) while the P-*M* bonds are equal (2.22 Å in CoP_3), giving rise to an almost tetrahedral coordination of P. In pure Si, the atoms are tetrahedrally coordinated with an interatomic distance of 2.35 Å and obviously covalently bonded. The similarities between the near-edge structures of the two compounds indicate strongly that the P atoms in skutterudites experience a similar covalent but semi-tetrahedral bonding arrangement. When comparing to the work by Garvie *et al.*[23,27] on Si in tetrahedral environments with different ligands and also the Si $L_{2,3}$ photoabsorption study by Waki and Hirai,[52] it is interesting to note how the present P spectra resemble that of pure Si rather than tetrahedrally coordinated Si in SiC or SiO_2. Waki and Hirai studied the effect of electronegativity of ligands surrounding tetrahedrally coordinated Si atoms on the Si $L_{2,3}$ photoabsorption spectrum. Their results from studies of Si, SiC, and SiO_2 show that more electronegative ligands produce spectra with stronger peaks than the less electronegative ligands. Thus the strongest initial peak was observed for SiO_2, intermediate for SiC, and weakest for elemental Si as expected from charge-transfer considerations based on the electronegativities in Table I.

TABLE I. Free-atom electronegativity values χ of relevant atomic species in Pauling units.

Atom	P	Co	Rh	Ir	Fe	Ni	Si	O	C
χ	2.1	1.8	2.2	2.2	1.8	1.8	1.8	3.4	2.6

We observe a similar trend for P in the skutterudites. With increasing electronegativity of the two surrounding *M* atoms, the peak at the edge threshold increases. Table I and Fig. 3 show that CoP_3 and NiP_3 with the lowest electronegativity for the *M* atoms have less pronounced peaks than RhP_3 and IrP_3.

Garvie and Buseck[27] show in their $L_{2,3}$ ELNES spectrum of P in PO_4 tetrahedral environments that there is a small prepeak (in their paper denoted A) not found in the present spectra. To explain this difference, we look closer at the study by Waki and Hirai[52] on Si $L_{2,3}$ photoemission spectra. They find that their peak corresponding to our peak A1 is distinctively lower in both width and height as the electronegativity of the ligand decreases. Thus, as the electronegativity of O is significantly higher than that of P and the *M* atoms in the skutterudites (Table I), it is to be expected that this peak is not well resolved in the skutterudites.

Comparing the spectra from $LaFe_4P_{12}$ and CoP_3, the peak A is more pronounced in $LaFe_4P_{12}$ than in CoP_3. From a simple electron count, $LaFe_4P_{12}$ has one electron less per $[LaFe_4P_{12}]$ unit than its CoP_3 counterpart: Assuming P closed-shell configuration, $M^{3+}[P_3]^{3-}$ is expected for binary skutterudites with the metal in d^6 $(t_{2g}^6 e_g^0)$ octahedral coordination.[16] In the ternary skutterudite $LaFe_4P_{12}$, an expected La valence state of La^{3+} gives $[Fe_4P_{12}]^{3-}$, compensating only for three of the four less electrons provided by Fe as compared to Co. Thus, a hole is expected either at one of the Fe atoms, resulting in a mixed Fe^{2+} and Fe^{3+} valence state or shared by the P atoms yielding a $P^{11/12-}$ state or hole in the valence band. The higher peak A in the $LaFe_4P_{12}$ spectrum indicates that the hole is situated at least partially on the P atoms, as suggested by Jung *et al.*[10] and by both Mössbauer[53] and XPS measurements[17] finding only Fe^{2+}. This is also in agreement with a previous EELS study of the metal $L_{2,3}$ edges of CoP_3 and $LaFe_4P_{12}$ (Ref. 20) and a recent theoretical charge-density study of the same materials,[54] showing that the main change upon adding La to the system is local around the phosphorus ion.

The filled skutterudite $LaFe_4P_{12}$ clearly differs from the binary skutterudites also in that the B feature is more or less absent. While the La $N_{4,5}$ edge extends well into the P $L_{2,3}$

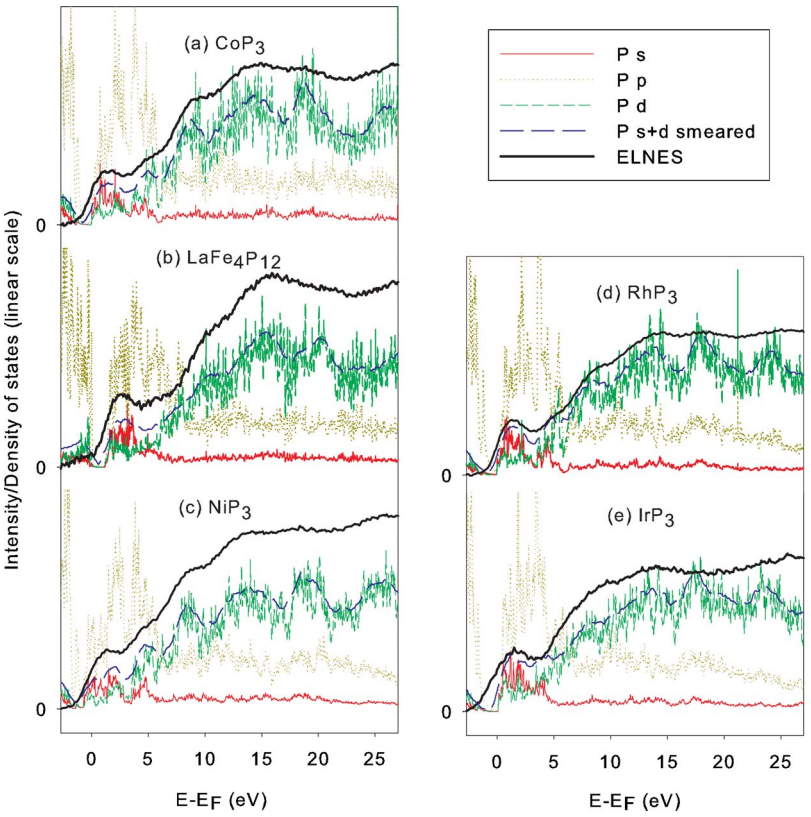

FIG. 4. (Color online) Comparison of experimental ELNES curves and electronic P *s*, *p* and *d* states from DFT calculations. From top to bottom: (a) CoP_3, (b) $LaFe_4P_{12}$, (c) NiP_3, (d) RhP_3, and (e) IrP_3. Experimental near-edge structure (thick/black line), P *s* (thin solid/red line), *p* (dotted/yellow line), and *d* (dot-dashed/green line) states. The thick-dashed/blue line shows the 1:1 sum of P *s* and *d* states smeared to an energy resolution of 1.5 eV.

peak region, we believe that the edge subtraction performed gives a reasonably accurate result as both the RSMS and DFT calculations confirm the absence of this feature. This difference between the spectra from the binary and ternary skutterudites thus probably reflects real changes in the bonding of the materials. One could speculate if the reason is P-La bonds that are created upon adding La to the system, as has also been suggested in Ref. 54.

It should be noted that all the calculated spectra presented here were simulated with a core hole in the 2*p* shell of the phosphorus atom, as this was found to give a better fit to the experimental data. Comparisons between spectra calculated with and without core hole reveal that peak A is highly sensitive to core-hole effects. When the core hole is accounted for, peak A is larger and more distinct. These differences can be traced back to changes in the local DOS of phosphorus above the Fermi level, where more *s* and *d* states are available in the conduction DOS when core-hole effects are present. This effect is larger in $LaFe_4P_{12}$ than in CoP_3 and may indicate a larger response of the valence electrons to the core hole for this compound.

Substituting Co for Ni transforms the CoP_3 semiconductor into the NiP_3 metal. Comparing the CoP_3 and NiP_3 spectra, the A1 peak is smeared out and pulled toward the Fermi level, thus generating the well-known metallic character in NiP_3. Note however the remarkable similarity between the CoP_3 and NiP_3 spectra, suggesting a very similar bonding and supporting the view that the extra electron added by Ni does not contribute to bonding to any significant degree.

Assuming that the dipole selection rule is valid, the $L_{2,3}$ edges represent transitions from occupied 2*p* states to empty states of *s* and *d* symmetry. Thus, a comparison to symmetry-projected local DOS should be able to explain the features seen experimentally. Figure 4 shows a comparison of the P *s* and *d* states as calculated by DFT with the experimental P $L_{2,3}$ edge. Also shown is the sum of P *s* and *d* states with a broadening of 1.5 eV. The broadening accounts for both experimental and intrinsic broadening effects. A summation of P *s* and *d* states in the ratio 1:1 is a crude approximation to the experimental edge; however the main features are well explained by this comparison. From the calculated DOS we see that the A and B features in the spectra result from transitions to hybridized *s* and *d* states above the Fermi level while the feature C results almost exclusively from transitions to empty *d* states.

Hansen *et al.*[55] have claimed that $L_{2,3}$ edges of tetrahedrally coordinated elements will inevitably, also under dipole approximation conditions, have a certain amount of *p* character due to centrosymmetry breaking in tetrahedral environments and mixing of electronic states to form sp^3 hybrid orbitals. They show this by comparing $L_{2,3}$ energy loss spectra from octahedral and tetrahedral Si and noting the difference in intensity of a peak $\sim 2-3$ eV above the Fermi energy. This would correspond to about the area of peak B in our skutterudite spectra. However, from our spectra and the calculated phosphorus *p* states, also shown in Fig. 4, we see that there is no such peak in this energy region or else in the spectrum that can be explained by introducing such $\Delta l=0$ transitions.

The P atoms in the skutterudites are not perfectly tetrahedrally coordinated, as each P atom has two P and two *M* neighbors at different interatomic distances. Normally such lowering of symmetry would reduce the degeneracy of the energy levels and cause the ELNES peaks to split. However,

we observe the same peaks as in perfectly tetrahedrally coordinated materials and thus conclude that the effect of splitting is too small to be visible. This is in agreement with earlier work on silicates,[27] finding that the effect of tetrahedral distortion is to broaden the peaks that would be present for the same material containing undistorted tetrahedra.[27]

The excited-state properties of the skutterudite compounds seem to be well described within the RSMS formalism as implemented in FEFF8 using spherical muffin-tin potentials and a local approximation of the exchange and correlation energy. While the DFT calculations in this work are semi-local and use a more sophisticated approximation of the exchange and correlation energies, there are no significant differences in the features predicted by the two approaches. It should also be noted that an accurate comparison of the DOS calculations with experiments require knowledge of the transition-matrix elements to weight the *s* and *d* states properly. However, the 1:1 weighting seems reasonable based on the good agreement between the calculations and experiments.

IV. CONCLUSIONS

In this study we have studied the experimental and calculated ELNES of various P containing skutterudites. Comparing the $L_{2,3}$ edges of P, it has been shown that the near-edge structure is very similar for all the investigated compounds, including the metallic NiP_3 and the metallic and filled skutterudite $LaFe_4P_{12}$. Many of the smaller differences between the compounds can be related to the electronegativity of the atoms in the structures, analogous with results from earlier work on Si $L_{2,3}$ edges. It is generally found that the P $L_{2,3}$ edges are similar to those of pure Si rather than those of other tetrahedrally coordinated Si compounds. RSMS calculations with core holes are able to reproduce the experimental spectra to a high degree for all the examined materials. Details in the near-edge structure are well explained by considering P *s* and *d* states without involving any *p* character states, as revealed by DFT electronic structure calculations.

ACKNOWLEDGMENTS

The authors wish to acknowledge Ole Bjørn Karlsen for preparing the materials and the Norwegian Research Council for financial support through the FRINAT project "Studies of electronic structure at the nanoscale."

*randi.holmestad@ntnu.no

[1] M. M. Koza, M. R. Johnson, R. Viennois, H. Mutka, L. Girard, and D. Ravot, Nature Mater. **7**, 805 (2008).
[2] M. Christensen, A. B. Abrahamsen, N. B. Christensen, F. Juranyi, N. H. Andersen, K. Lefmann, J. Andreasson, C. R. H. Bahl, and B. B. Iversen, Nature Mater. **7**, 811 (2008).
[3] G. S. Nolas, J. L. Cohn, and G. A. Slack, Phys. Rev. B **58**, 164 (1998).
[4] B. C. Sales, D. Mandrus, B. C. Chakoumakos, V. Keppens, and J. R. Thompson, Phys. Rev. B **56**, 15081 (1997).
[5] M. Christensen, B. B. Iversen, L. Bertini, C. Gatti, M. Toprak, M. Muhammed, and E. Nishibori, J. Appl. Phys. **96**, 3148 (2004).
[6] C. Stiewe, L. Bertini, M. Toprak, M. Christensen, D. Platzek, S. Williams, C. Gatti, E. Muller, B. B. Iversen, M. Muhammed, and M. Rowe, J. Appl. Phys. **97**, 044317 (2005).
[7] Z. Zhou, C. Uher, A. Jewell, and T. Caillat, Phys. Rev. B **71**, 235209 (2005).
[8] J. Yang, D. T. Morelli, G. P. Meisner, W. Chen, J. S. Dyck, and C. Uher, Phys. Rev. B **65**, 094115 (2002).
[9] H. Anno, K. Matsubara, Y. Notohara, and T. Sakakibara, J. Appl. Phys. **86**, 3780 (1999).
[10] D. W. Jung, M. H. Whangbo, and S. Alvarez, Inorg. Chem. **29**, 2252 (1990).
[11] M. Llunell, P. Alemany, S. Alvarez, V. P. Zhukov, and A. Vernes, Phys. Rev. B **53**, 10605 (1996).
[12] M. Fornari and D. J. Singh, Phys. Rev. B **59**, 9722 (1999).
[13] I. Lefebvre-Devos, M. Lassalle, X. Wallart, J. Olivier-Fourcade, L. Monconduit, and J. C. Jumas, Phys. Rev. B **63**, 125110 (2001).
[14] O. M. Lovvik and O. Prytz, Phys. Rev. B **70**, 195119 (2004).
[15] K. Takegahara and H. Harima, Physica B **328**, 74 (2003).
[16] C. Uher, Semicond. Semimetals **69**, 139 (2001).
[17] A. P. Grosvenor, R. G. Cavell, and A. Mar, Chem. Mater. **18**, 1650 (2006).
[18] A. P. Grosvenor, R. G. Cavell, and A. Mar, Phys. Rev. B **74**, 125102 (2006).
[19] S. Diplas, O. Prytz, O. B. Karlsen, J. F. Watts, and J. Taftø, J. Phys.: Condens. Matter **19**, 246216 (2007).
[20] O. Prytz, J. Taftø, C. C. Ahn, and B. Fultz, Phys. Rev. B **75**, 125109 (2007).
[21] V. J. Keast, A. J. Scott, R. Brydson, D. B. Williams, and J. Bruley, J. Microsc. **203**, 135 (2001).
[22] P. A. van Aken, B. Liebscher, and V. J. Styrsa, Phys. Chem. Miner. **25**, 323 (1998).
[23] L. A. J. Garvie, A. J. Craven, and R. Brydson, Am. Mineral. **79**, 411 (1994).
[24] J. Taftø and J. Zhu, Ultramicroscopy **9**, 349 (1982).
[25] R. D. Leapman and J. A. Hunt, Microsc. Microanal. Microstruct. **2**, 231 (1991).
[26] M. A. Aronova, Y. C. Kim, G. Zhang, and R. D. Leapman, Ultramicroscopy **107**, 232 (2007).
[27] L. A. J. Garvie and P. R. Buseck, Am. Mineral. **84**, 946 (1999).
[28] S. Miao, M. Kocher, P. Rez, B. Fultz, R. Yazami, and C. C. Ahn, J. Phys. Chem. A **111**, 4242 (2007).
[29] W. Jeitschko, A. J. Foecker, D. Paschke, M. V. Dewalsky, C. B. H. Evers, B. Kunnen, A. Lang, G. Kotzyba, U. C. Rodewald, and M. H. Moller, Z. Anorg. Allg. Chem. **626**, 1112 (2000).
[30] A. Watcharapasorn, R. C. DeMattei, R. S. Feigelson, T. Caillat, A. Borshcevsky, G. J. Snyder, and J.-P Fleurial, J. Appl. Phys. **86**, 6213 (1999).
[31] W. Jeitschko and D. Brown, Acta Crystallogr. B **33**, 3401

(1977).
[32] A. L. Ankudinov, B. Ravel, J. J. Rehr, and S. D. Conradson, Phys. Rev. B **58**, 7565 (1998).
[33] L. Hedin and B. I. Lundqvist, J. Phys. C **4**, 2064 (1971).
[34] D. C. Langreth and M. J. Mehl, Phys. Rev. B **28**, 1809 (1983).
[35] A. D. Becke, Phys. Rev. A **38**, 3098 (1988).
[36] J. P. Perdew, J. A. Chevary, S. H. Vosko, K. A. Jackson, M. R. Pederson, D. J. Singh, and C. Fiolhais, Phys. Rev. B **46**, 6671 (1992).
[37] J. P. Perdew, J. A. Chevary, S. H. Vosko, K. A. Jackson, M. R. Pederson, D. J. Singh, and C. Fiolhais, Phys. Rev. B **48**, 4978(E) (1993).
[38] P. E. Blöchl, Phys. Rev. B **50**, 17953 (1994).
[39] G. Kresse and D. Joubert, Phys. Rev. B **59**, 1758 (1999).
[40] J. P. Perdew, K. Burke, and M. Ernzerhof, Phys. Rev. Lett. **77**, 3865 (1996).
[41] G. Kresse and J. Hafner, Phys. Rev. B **48**, 13115 (1993).
[42] G. Kresse and J. Hafner, Phys. Rev. B **49**, 14251 (1994).
[43] G. Kresse and J. Furthmüller, Comput. Mater. Sci. **6**, 15 (1996).
[44] G. Kresse and J. Furthmüller, Phys. Rev. B **54**, 11169 (1996).
[45] VASP code, http://cms.mpi.univie.ac.at/vasp/
[46] P. Pulay, Chem. Phys. Lett. **73**, 393 (1980).
[47] A. D. Vita, Ph.D. thesis, Keele University, 1992.
[48] P. E. Blöchl, O. Jepsen, and O. K. Andersen (unpublished).
[49] B. Cordero, V. Gómez, A. E. Platero-Prats, M. Revés, J. Echeverría, E. Cremades, F. Barragán, and S. Alvarez, Dalton Trans **2008**, 2832.
[50] O. Prytz and E. Flage-Larsen (unpublished).
[51] C. C. Ahn and O. L. Krivanek, *EELS Atlas* (Gatan, Warrendale, 1983).
[52] I. Waki and Y. Hirai, J. Phys.: Condens. Matter **1**, 6755 (1989).
[53] G. K. Shenoy, D. R. Noakes, and G. P. Meisner, J. Appl. Phys. **53**, 2628 (1982).
[54] E. Flage-Larsen, O. M. Løvvik, O. Prytz, and J. Taftø (unpublished).
[55] P. L. Hansen, R. Brydson, and D. W. McComb, Microsc. Microanal. Microstruct. **3**, 213 (1992).